Temperature Sensor Based on Fiber Bragg Grating Embedded in SNS Fiber Structure

Yuan Huiying[1], *Zeng Jie*[1*], *Li Ming*[2], *Si Yawen*[1], *Zheng Dingwu*[1], *Liu Zhe*[1], *He Wanwan*[1], *Huang Jukun*[1]

1. State Key Laboratory of Mechanics and Control of Mechanical Structures, Nanjing University of Aeronautics and Astronautics, Nanjing 210016, P. R. China;
2. AVIC China Aero-Polytechnology Establishment, Beijing 100028, P. R. China

(Received 20 September 2017; revised 10 May 2018; accepted 20 May 2018)

Abstract: A novel fiber temperature sensor based on multimode interference theory is proposed and experimentally demonstrated. The sensing head is formed by a fiber bragg grating (FBG) connected with single-mode-no core-single-mode fiber(SNS) fiber structure which consists of two sections of single mode fiber and no-core fiber . Using such a structure, not only the reflective measurement can be realized, but also the need for a gold-plated film can be avoided at the end of the fiber to enhance the reflected light signal. More importantly, the sensitivity is increased by 4 times as compared with the conventional FBG temperature sensor according to the experimental results, and it also provides the development space for multi-parameters monitoring.

Key words: fiber bragg grating; no-core fiber; multimode interference; temperature monitoring

CLC number: TN253 **Document code**: A **Article ID**: 1005-1120(2018)S-0046-05

0 Introduction

As an extremely important kind of optical fiber sensor, optical fiber interference sensor has the advantages of high resolution, high precision and high dynamic range [1-3]. Compared to fiber grating sensors, the fiber optic interference sensor is more compact, smaller, and more accurate to measure, which is suitable for applications where the installation location is small or the sensor integration requirements are high. In recent years, a simple single-mode-multimode -single-mode (SMS) optical fiber structure has attracted a lot of attentions, and the transmission-type of SMS fiber structure is used by most researchers [4-5], which has been widely used to monitor temperature, strain, displacement, humidity and other parameters [6-9]. The optical fiber sensing portion is placed in an environment to be measured for sensing, which makes it has some limitations in many applications and it is inconvenient to operate. Moreover, the conventional SMS structure needs to use hydrofluoric acid to chemically etch the cladding of the multimode fiber, and even corrode the core of the multimode fiber. It is not only dangerous, but also difficult to precisely control. So this paper uses the no-core fiber (NCF) as the SMS structure of the multimode waveguide part. And the reflection-type SMS structure, since the optical signal reflected from the end of the untreated fiber is weak, a reflecting device (a gold film or a reflective mirror, etc.) is usually designed on the end face of the fiber sensing part, so that the cost is high and difficult to operate [10].

For the above problems, in this paper, a novel and high sensitivity temperature sensor based on a FBG connected to a section of NCF is demonstrated. Additionally, NCF is used as the multimode waveguide in SMS structure, the NCF acts as the fiber core and the external medium acts as the fiber cladding when it is in use, so that

* Corresponding author, E-mail address: zj2007@nuaa.edu.cn

How to cite this article: Yuan Huiying, Zeng Jie, Li Ming, et al. Temperature sensor based on fiber bragg grating embedded in SNS fiber structure[J]. Trans. Nanjing Univ. Aero. Astro., 2018,35(S):46-50.
http://dx.doi.org/10.16356/j.1005-1120.2018.S.046

the external environment can be directly perceived, which makes it more sensitive to the changes of the ambient temperature.

Combining SNS fiber structure with fiber Bragg grating, not only can improve the sensitivity, avoid the complexity of coating process, and no need to corrode the fiber Bragg grating diameter to the nanometer level which will reduce its mechanical strength, but also can achieve reflection measurement, and is beneficial to miniaturize and encapsulate the sensor.

1 Principle and Modeling of Sensor

The schematic diagram of the FBG embedded in the SNS fiber structure is shown in Fig. 1.

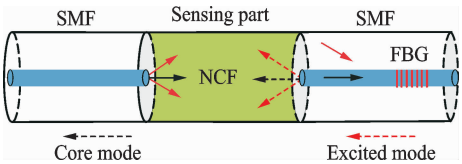

Fig. 1. Schematic diagram of sensor

The basic principle is a number of higher order modes will be excited when the light is coupled into the NCF from the incident single-mode fiber, these modes are coupled to each other and transmitted to the output single-mode fiber, when transmitted to the FBG embedded, the optical signal which satisfies the Bragg condition [11] will be reflected back to the NCF again. Due to the interference phenomenon between low and high modes, the reflection spectrum will appear peaks or troughs, and both the mode interference signal of the SNS structure and the reflected signal of the FBG are included in the reflection spectrum of the SNS-FBG structure which can be used to realize the monitor of ambient temperature.

When the light propagates along the single-mode fiber (SMF) into the NCF, different high modes can be excited in the NCF and supported by the NCF because of its large radius. Assuming that SMF and the NCF have circular cross sections and step index distributions, only linear polarized radial modes LP_{0m} modes (m is a positive integer) will be excited and transmitted in the NCF [12-13]. The mode field of LP_{0m} mode can be expressed as follows

$$E_m(r) = c_m J_0(u_m r)\exp(-\mathrm{i}\beta_m z) \tag{1}$$

Where J_0 is the Bessel function of the zero order, β_m is the longitudinal propagation constant, u_m is the normalized transverse propagation constant of the fiber core, c_m is the excited coefficient, which can be written as

$$c_m = \frac{\int_0^{\infty} E_m(r)E_s(r)r\mathrm{d}r}{\left[\int_0^{\infty}|E_m(r)|^2 r\mathrm{d}r\int_0^{\infty}|E_s(r)|^2 r\mathrm{d}r\right]^{1/2}} \tag{2}$$

Where $E_s(r)$ is the mode field of LP_{01} mode in the SMF, it can be approximated as a Gaussian beam.

When the length of NCF is L, the output electric filed distribution can be written as

$$E(r) = \sum_{m=1}^{N} c_m J_0(u_m r)\exp(-\mathrm{i}\beta_m L) \tag{3}$$

Thus the output power of the modal interference is

$$I(r) = E(r)E^*(r) = \sum_{m=1}^{N}\sum_{n=1}^{N} c_m c_n^* \varphi_m(r)\varphi_n^*(r)\exp[-\mathrm{i}(\beta_m - \beta_n)L] \tag{4}$$

Since the FBG has been written in the output single-mode fiber, when the Bragg reflection condition is satisfied, high order modes and the fundamental core mode are partially reflected into the NCF again and will output in the beginning SMF.

From the above formulas, it can be known that the energy coupling coefficient determines the magnitude of the excitation modes power. By solving the coupling coefficient, the optical power of each order mode can be calculated, and the interference between modes can be established. The bigger the optical energy at the end of the NCF, the stronger the optical signal coupled to the output SMF, and the greater the reflected light signal. When the input light wavelength and the fiber structure are constant, the output intensity is related to the length of the NCF [14]. Therefore, in order to obtain the maximum output signal intensity, the optical field distribution in the NCF is simulated by Rsoft. In the simulation the incident wavelength is the center wavelength of the FBG used in this study, which is 1 552.05 nm, and the refractive index of NCF is 1.463 with a diameter of 125 μm, the core radius of SMF is

4.2 μm with a cladding diameter of 125 μm. The simulation result is shown in Fig. 2.

According to Fig. 2 (a), the energy distribution of the optical field remains at 1 when the light propagates in SMF, and there are multiple excited modes in NCF, coupling between each other which results in weakening or superposition of energy along the NCF. And in Fig. 2 (b), the energy of some transmission points in NCF is very large, and the energy at some transmission points is very small, and the distribution of the light field in the direction of the transmission distance occurs periodically, that is, namely the self-image effect. According to Ref. [15], the fourth self-imaging exhibits the lowest insertion loss compared to the other imaging, so the optimum length of the NCF can be chosen to improve the sensitivity of the sensor.

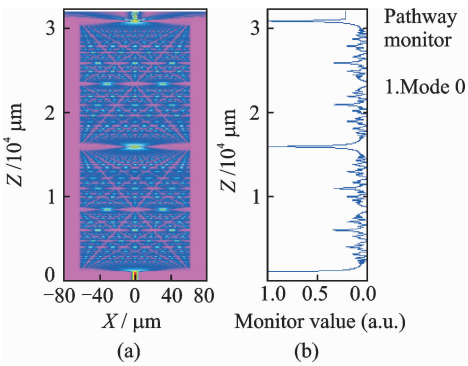

Fig. 2 Light field distribution of SNS structure

Based on the results of simulation, a NCF with a length of 6 cm is used to make the sensor. According to Ref. [16], when the ambient temperature rises, the maximum or the minimum wavelength of the interference of the reflection spectrum will move toward the long wave, and the wavelength changes linearly monotonically with temperature. Thus temperature can be monitored by studying the change of interference wavelength.

2 Experiment and Discussion

The reflection-type fiber temperature monitoring system based on SNS structure and FBG is shown in Fig. 3.

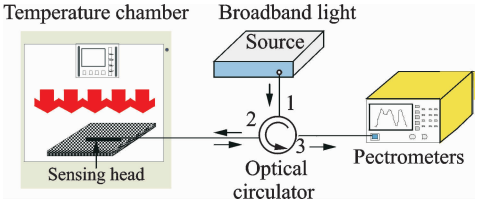

Fig. 3 Schematic diagram of experimental system

The system consists of ASE broadband light source, AQ6317C spectrum analyzer (spectral resolution 0.01nm), optical circulator, and Challenge-CH250C environmental test chamber and so on. The role of the optical circulator is to make light unidirectional transmission, the broadband light source enters from the port 1 and transmitted from the port 2 to the sensing probe, and then the reflected light signal is transmitted to the spectrometer from the port 3, thus the reflection spectra of the sensor in different temperatures can be obtained by the spectrometer, finally be processed and analyzed by a computer.

During the experiment, the prepared sensor was fixed straight on the plexiglass, and then the encapsulated sensor was placed in the environmental test chamber, the temperature range is from 40 to 100℃, measured every 10℃. Attention, in order to prevent the structure from being heated unevenly and cause negative effects on the experimental results, each temperature monitoring point needs to be kept warm for a period of time. The reflection spectrum obtained from the spectrometer is shown in Fig. 4.

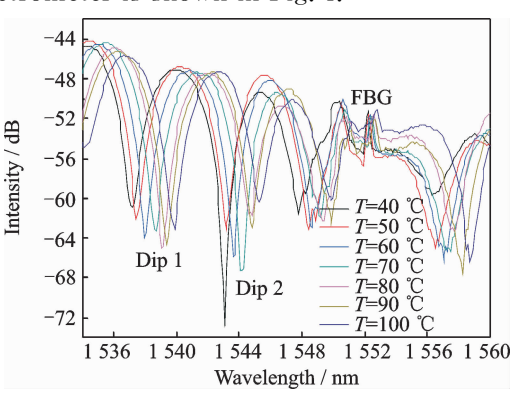

Fig. 4 Reflection spectrum of the sensor to temperature

From Fig. 4, it can be seen that both the SNS structure and FBG undergo red shift with the increase of temperature, which is consistent with previous theoretical results. The interfer-

ence fringes of the reflection spectrum are in good shape, indicating that the SNS-FBG fiber sensor has better temperature sensing characteristics, so it can be used to measure the temperature accurately. And there are two obvious interference dips in the range of the entire wavelength that can be chosen as the characteristic wavelengths, which are labeled as dip1 and dip2, respectively. At last, the comparison and analysis between the two dips and the FBG is carried out separately about the temperature responses (Fig. 5,6).

Due to the thermal expansion effect and the coupling effects of multimode interference, the reflection peak of FBG changes from 1 552.1 nm to 1 552.8 nm in the scope of temperature, and the temperature sensitivity is 0.011 7 nm/℃. And the wavelength at dip1 shifts 2.7 nm toward the long wave direction, so the temperature sensitivity is 0.045 nm/℃, It's about 4 times as good as FBG, and has a good linearity.

Similarly, the wavelength at dip2 moves to the long wave direction of 2.1 nm, which has a temperature sensitivity of 0.035 nm/℃, It's about 3 times as good as FBG, also has a good linearity.

Above all, The experimental results show that the SNS structure embedded with FBG can effectively improve the sensitivity of temperature measurement.

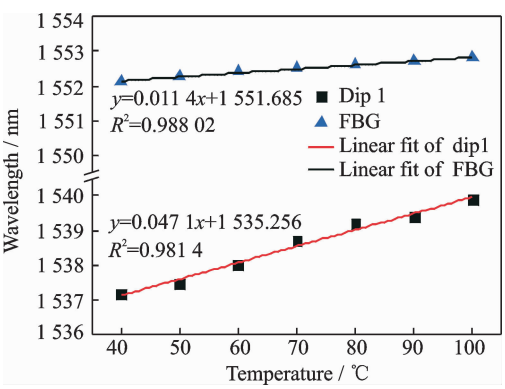

Fig. 5 Temperature response curves at FBG and Dip1

3 Conclusions

A reflective temperature sensor with fiber Bragg grating (FBG) embedded in SNS fiber structure is proposed, not only realizes the reflective measurement, extends its application field, but also avoids the trouble of coating process. The feasibility of this method is proved by comparing the experimental results with the theoretical results. The experimental results show that there are many interference dips in the whole reflection spectrum due to the influence of multimode interference, and the wavelength at dips shifts toward the long wave with the increase of the ambient temperature.

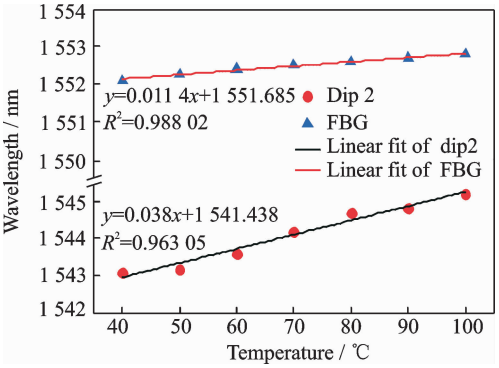

Fig. 6 Temperature response curves at FBG and Dip2

Compared with the individual FBG temperature sensor, the temperature sensitivity of the sensor is improved by about 4 times in the temperature range of 40～100 ℃. So the structure can effectively improve the temperature sensitivity, and the sensor has the advantages of simple manufacture, convenient operation, easy to implant and easy to miniaturization, can be used for temperature measurement and structural health monitoring of large structures, and composite materials in aircraft.

Acknowledgements

This work was supported by the National Natural Science Foundation of China (No. U1537102), the Fund of Aeronautics Science (No. 20152852036,20170252004), the Fundamental Research Funds for the Central Universities (NS2016004), the Shanghai Academy of Spaceflight Technology (No. SAST2015062), and the State Key Laboratory of Mechanics and Control of Mechanical Structures (Nanjing University of Aeronautics and astronautics)(No. MCMS-0516K01)

References:

[1] ZENG J, WANG W J, WANG B, et al. Sensitivity of optical FBG sensor under dynamic/static load in Chinese [J]. Journal of Nanjing University of Aero-

nautics & Astronautics, 2015, 47(3):397-403.
[2] RONG Q Z,QIAO X G, WANG R H, et al. High-sensitive fiber optic refractormeter based on a core-diameter-mismatch Mach-Zehnder interferometer [J]. IEE Sensors Journal, 2012, 12(7):2501-2505.
[3] XU Y, WANG D X, TANG T Y, et al. Debonding patch detection in FRP-strengthened materials with fiber-optic interferometer [J]. Transactions of Nanjing University of Aeronautics and Astronautics, 2017, 34(3):254-265.
[4] ZHOU D P, LI W, LIU W K, et al., Simultaneous measurement for strain and temperature using fiber Bragg gratings and multimode fibers [J]. Applied Optics, 2008, 47(10): 1668-1672.
[5] MA L, KANG Z X, QI Y H, et al. Fiber-optic temperature sensor based on a thinner no-core fiber[J]. Optik, 2015, 126: 1044-1046.
[6] Tripathi Saurabh M, Kumar A. Strain and temperature sensing characteristics of Single-mode Multimode-Single-mode structure [J]. Journal of lightwave Technology,2009,27(12):2348-2356.
[7] LI E B, WANG X L, ZHANG C, et al. Fiber-optic temperature sensor based on interference of selective higher-order modes [J]. Applied Physics letters, 2006, 89(9):369-449.
[8] Arifini A, Hatta A M, Sekartedjo K, et al. Long-range displacement sensor based on SMS fiber structure and OTDR [J]. Photonic Sensors, 2015,5(3): 166-171.
[9] SHAO M, QIAO X G, FU H W, et al. Fiber humidity sensor based on fiber bragg grating sandwiched in SMS [J] Spectroscopy and Spectral Analysis, 2016, 36(9): 3008-3013.
[10] ZHOU X L, CHEN K, MAO X F, et al. A reflective fiber-optic refractive index sensor based on multimode interference in a coreless fiber [J]. Optics Communications,2015,340:50-55.
[11] WU Q, Semenova Y, YAN B, et al. Fiber refractometer based on a fiber Bragg grating and single-mode multimode single-mode fiber structure [J] . Optics Letters,2011, 36(12): 2197-2199.
[12] Arum K, Ravi K V, Siny A C, et al. Transmission characteristics of SMS fiber optic sensor structures [J]. Optic Communications,2003,219(1):215-219.
[13] Soldano L B, Erik C, Pennings M. Optical multimode interference devices based on self-imaging: Principles and applications [J]. Lightwave Technology, 1995, 13(4): 615-627.
[14] LI Y, LIU Y, LIU Z B, et al. A refractive index sensor based on single-mode no-core single-mode fiber structure [J]. Journal of Optoelectronics Laser, 2013, 24(7): 1280-1285.
[15] Castillo-Guzman A. Widely tunable erbium-doped fiber laser based on multimode interference effect [J]. Opt Express, 2010,18(12): 591-597.
[16] WANG W, LI E B, ZHANG C L, et al. Simulation and experimental studies of multimode interference based fiber-optic temperature sensors [J]. Journal of Optoelectronics Laser,2008, 19(12): 1572-1575.

Ms. **Yuan Huiying** received a master's degree in test and measurement technology and instrumentation from Nanjing University of Aeronautics and Astronautics in 2018. Her research focuses on coreless fiber sensing.

Dr. **Zeng Jie**is an associate professor and master tutor of State Key Laboratory of Mechanical Structural Mechanics and Control, Nanjing University of Aeronautics and Astronautics. More than ten national invention patents have been applied for or authorized. He is a member of the Chinese Aviation Society. His main research directions are intelligent material and structural health monitoring and new optical fiber sensing technology.

Dr. **Li Ming** graduated from the School of Materials Science and Engineering, Beihang University, majoring in materials physics and chemistry. Now he is working as a Senior Engineer at China Aviation Integrated Technology Research Institute. His main research interest is aviation product corrosion protection and control.

Mr. **Si Yawen** obtained a bachelor's degree in information engineering from China University of Mining and Technology in 2016. He is currently pursuing a master's degree in test metrology technology and instrumentation at Nanjing University of Aeronautics and Astronautics. His current research focus is deformation monitoring.

Mr. **Zheng Dingwu** obtained a bachelor's degree in information engineering from China University of Mining and Technology in 2016. He is currently pursuing a master's degree in test metrology technology and instrumentation at Nanjing University of Aeronautics and Astronautics. His current research focuses on impact location and monitoring.

Mr. **Liu Zhe** received a bachelor's degree in aircraft design and engineering from North University of China in 2016. He is currently pursuing a master's degree in aeronautical engineering from Nanjing University of Aeronautics and Astronautics. His current research focuses on structural health monitoring.

Ms. **He Wanwan** was awarded a bachelor's degree in measurement and control technology and instrumentation from Anhui University of Engineering in 2016. She is currently pursuing a master's degree in test metrology technology and instrumentation at Nanjing University of Aeronautics and Astronautics. Her current research focuses on impact location and monitoring of flexible structures.

Mr. **Huang Jukun** received a bachelor's degree from Nanchang Aviation University in 2016. He is currently pursuing a master's degree in aeronautical engineering from Nanjing University of Aeronautics and Astronautics. His current research focuses on strain field reconstruction.

(Production Editor: Chen Jun)